Minireview

Emerging views on the structure and dynamics of the Ca^{2+}-ATPase in sarcoplasmic reticulum

Anthony N. Martonosi, Istvan Jona, Elek Molnar, Norbert W. Seidler, Rene Buchet and Sandor Varga

Department of Biochemistry and Molecular Biology, State University of New York, Health Science Center, Syracuse, NY 13210, USA

Received 14 May 1990

The ATP-dependent Ca^{2+} transport in sarcoplasmic reticulum involves transitions between several structural states of the Ca^{2+}-ATPase, that occur without major changes in the secondary structure. The rates of these transitions are modulated by the lipid environment and by interactions between ATPase molecules. Although the Ca^{2+}-ATPase restricts the rotational mobility of a population of lipids, there is no evidence for specific interaction of the Ca^{2+}-ATPase with phospholipids. Fluorescence polarization and energy transfer (FET) studies, using site specific fluorescent indicators, combined with crystallographic, immunological and chemical modification data, yielded a structural model of Ca^{2+}-ATPase in which the binding sites of Ca^{2+} and ATP are tentatively identified. The temperature dependence of FET between fluorophores attached to different regions of the ATPase indicates the existence of 'rigid' and 'flexible' regions within the molecule characterized, by different degrees of thermally induced structural fluctuations.

Ca^{2+}-ATPase; Sarcoplasmic reticulum; Energy transfer; Electron microscopy

1. INTRODUCTION

The mechanism of coupling between ATP hydrolysis and Ca^{2+} transport is determined by the spatial relationship of the phosphorylation and ATP binding domains of the Ca^{2+}-ATPase to the Ca^{2+} channel involved in the translocation of calcium. Two alternative coupling mechanisms have been proposed, based on two rather different hypothetical models of the structure of the Ca^{2+}-ATPase. In the 'conformational coupling' mechanism the utilization of the free energy of ATP hydrolysis for Ca^{2+} transport involves a mechanical coupling over long distances between physically separate ATP binding and Ca^{2+} transport sites [1], while in the 'ligand conduction' mechanism a direct interaction is postulated between the phosphoryl group of ATP and the transported calcium [2–4].

The conformational coupling hypothesis is supported by the existence of at least two structurally distinct conformational states of the Ca^{2+}-ATPase (E_1 and E_2) that differ in their affinities and vectorial specificities for ATP, P_i, and Ca^{2+} [5,6]. Evidence obtained by chemical modification, site-specific mutagenesis, and intramolecular energy transfer suggests that the site responsible for the binding of ATP is located in the cytoplasmic domain of the Ca^{2+}-ATPase [7], while the high affinity Ca^{2+} binding sites are presumed to be within the lipid bilayer [8]. The estimated distance of ~20–40 Å between these two sites would make conformational change an obligatory element of the coupling process. However, due to the scarcity of independent structural information and uncertainties about the localization and orientation of some of the probes used for energy transfer measurements, the current estimates of intramolecular distances are only tentative. The conformational changes associated with $E_1 \longrightarrow E_2$ transition [9] appear

Correspondence address: A.N. Martonosi, Department of Biochemistry and Molecular Biology, State University of New York, Health Science Center, Syracuse, NY 13210, USA

Abbreviations: ANS, 8-anilinonaphthalene sulfonate; DPH, diphenylhexatriene; FITC, fluorescein-5'-isothiocyanate; FRET, Forster resonance energy transfer; IAEDANS, 5'(2-((iodoacetyl)-amino)ethyl)aminonaphthalene-1-sulfonic acid; AEDANS, covalently bound IAEDANS; FCD, fluorescent carbodiimide derivatives; RITC-DPPE, rhodamine-5'-isothiocyanyl-dipalmitoylphosphatidylethanolamine; SR, sarcoplasmic reticulum; TNP-N, trinitrophenyl nucleotide; TNP-ATP, trinitrophenyl ATP; TNP-AMP, trinitrophenyl AMP

Published by Elsevier Science Publishers B.V. (Biomedical Division)
00145793/90/$3.50

to involve surprisingly small changes in the secondary structure of the Ca^{2+}-ATPase [10–13], and in the intramolecular distances determined by energy transfer [14,15], that may actually favor the direct coupling mechanism.

Our studies, using crystallographic [16–19], spectroscopic [10,11,13,15,20,21], immunological [22] and chemical modification [23] techniques are aimed at localizing the structural changes connected with E_1–E_2 transition in the three-dimensional structure of the Ca^{2+}-ATPase, and at clarifying their relationship to Ca^{2+} transport.

2. THE ANALYSIS OF Ca^{2+}-ATPase CRYSTALS

The Ca^{2+}-ATPase can be crystallized in the presence of Ca^{2+} or lanthanides in the E-Ca^{2+} or E-La^{3+} state, previously identified as the E_1 state [17,19]. The enzyme can also be crystallized in the absence of Ca^{2+} by the addition of vanadate or inorganic phosphate in he E-V or E-P_i conformation, earlier identified as the E_2 state [16–19]. The unit cell of the E-La^{3+} crystals is monomeric, with a space group of P1 [17], while the E-V crystals have dimeric unit cells with a space group of P2 [18]. The projection maps indicate major differences in the spatial relationship of the ATPase molecules in the two crystal forms, but the pear-shaped cytoplasmic profile of the Ca^{2+}-ATPase is similar, at ~25 Å resolution, in the two types of crystals.

There are three types of interactions between Ca^{2+}-ATPase molecules in the E-V crystals.

(A) The dimeric structural units are stabilized by massive protein *bridges* (marked 'A' in Fig. 1) that link the cytoplasmic domains of two ATPase molecules into an antiparallel dimer [18]; Ca^{2+} in μmol concentration breaks these bridges and causes the rearrangement of ATPase molecules into P1 type crystals stabilized by Ca^{2+} [17]. The Ca^{2+} sensitivity indicates that the ligand specificity of the Ca^{2+}-ATPase in the E-V crystals resembles that of the E·P state stabilized by inorganic phosphate [5,6].

(B) Further contacts between the lobe region of one ATPase molecule and the head region of the next

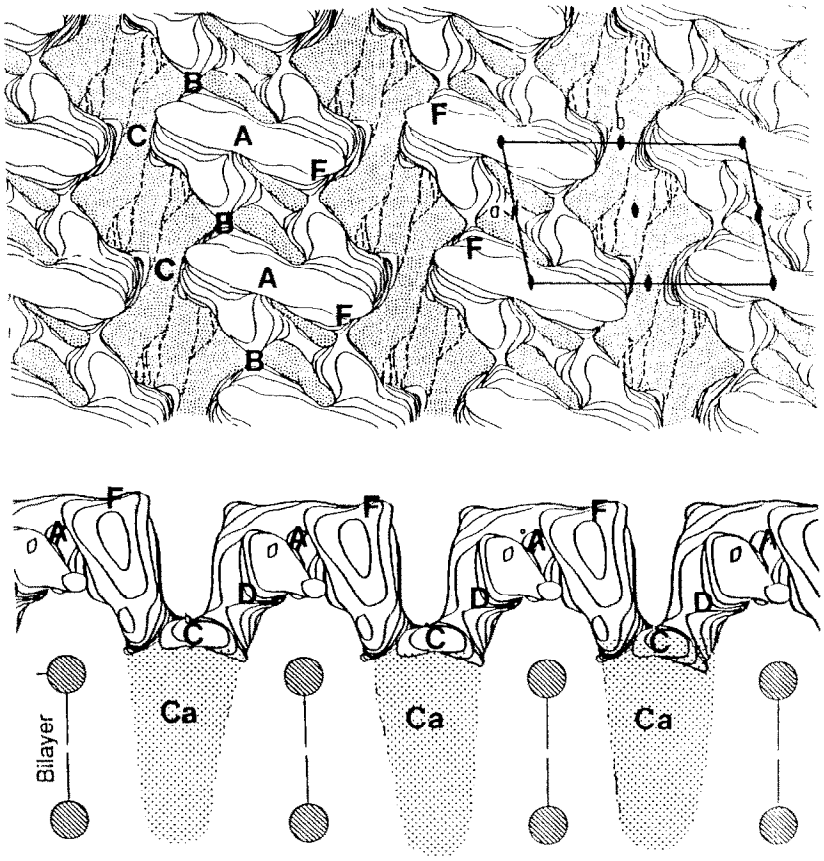

Fig. 1. The structure of the Ca^{2+}-ATPase at ~25 Å resolution. The surface contours of the Ca^{2+}-ATPase obtained by electron microscope reconstructions of vanadate-induced E_2V type crystals are viewed normal to the membrane plane (top panel) and from within the membrane plane (bottom panel) based on the data of Taylor et al. [18]. In the top panel the unit cell indicated by lines 'a' and 'b' contains an ATPase dimer. The principal contact regions between the ATPase molecules in the lattice are marked by 'A', 'B', and 'C', as described in the text. The putative binding sites for FITC, AEDANS and Ca^{2+} are indicated by 'F', 'D' and 'Ca', respectively. The binding site for mAb A52 is tentatively assigned to the 'D', while that of anti-FITC to the 'F' region. Reproduced from [22].

(marked 'B' in Fig. 1), link the ATPase dimers into dimer chains.

(C) Finally contacts exist, within the bilayer, between ATPase molecules in adjacent dimer chains (marked 'C' in Fig. 1) that stabilize the crystal lattice. Interference with the C-type interactions explains the disruption of the E-V crystals by detergents [24].

The Ca^{2+} binding domain is presumed to be located at sites marked 'Ca' in Fig. 1 near the center of the bilayer; the tentative location of the ATP binding site is in the head portion of the cytoplasmic domain near the bridge at a position marked 'F' in Fig. 1 [15,22], based on the labeling of the ATP binding site by FITC [7]. The height of the ATPase molecule above the surface of the bilayer is ~60 Å and its overall length including the membrane-embedded portion is close to 100 Å.

3. THE EFFECT OF ANTI-ATPase ANTIBODIES

The effects of 14 monoclonal and 5 polyclonal antibodies on the enzymatic activity and interactions of the Ca^{2+}-ATPase were analyzed [22]. Most of the antibodies with epitopes on the B tryptic fragment (residues 506–1001) reacted with the native enzyme, indicating that this region of the molecule is highly accessible; by contrast, 5 out of 6 antibodies directed against the A_1 region of the Ca^{2+}-ATPase (residues 199–505) were reactive only after solubilization or denaturation of the enzyme. The B region contains part of the ATP binding domain, while the A_1 region contains the phosphate acceptor Asp-351 [7]. The epitope of the monoclonal antibody A52 is at residues 659–668 adjacent to the AEDANS binding site at cysteine 670–674 (tentatively marked 'D' in Fig. 1).

The A52 antibody interfered with the crystallization of Ca^{2+}-ATPase in the presence of vanadate and decreased the stability of preformed Ca^{2+}-ATPase crystals. We propose that the A52 epitope is located near the B-type contacts between the head and lobe regions of the ATPase molecule (marked 'D' in Fig. 1), and we attribute the disruption of the Ca^{2+}-ATPase crystals by A52 to interference with the B-type interactions [22]. The effect of A52 is highly specific and not shared by 5 other monoclonal antibodies that bind to the C-terminal domain of the native Ca^{2+}-ATPase.

4. INTRAMOLECULAR DISTANCES DETERMINED BY FLUORESCENCE ENERGY TRANSFER

The shape and dimensions of the ATPase molecule determined by the 3D reconstruction of 2-dimensional Ca^{2+}-ATPase crystals (Fig. 1) can be compared with the intramolecular distances determined by energy transfer between fluorophores bound at specified locations within the ATPase molecule [14,15,25–33]. Several of these distances are subject to considerable uncertainty, and should be used only as approximate indicators of the relative positions of the various sites within the ATPase molecule.

The two high affinity Ca^{2+} sites are probably within 10 Å of each other [25,26]. Their localization within the bilayer is supported by the observation [8] that site-specific mutagenesis of several amino acids within the putative transmembrane helices interferes with Ca^{2+} binding and with the Ca^{2+}-dependent phosphorylation of the enzyme by ATP, but has no effect on the Ca^{2+}-independent phosphorylation by inorganic phosphate. The energy transfer between Tb^{3+} and RITC-DPPE [27] and the quenching of the fluorescence of carbodiimides attached to the putative Ca^{2+} site by doxylstearates [25] places the Ca^{2+} site near the middle of the bilayer.

The estimated distances between lanthanides bound at various cation binding sites on the Ca^{2+}-ATPase, and FITC, TNP-AMP, and Cr-ATP bound at the nucleotide binding site range between 10 and 47 Å [26,28–31].

The longer distances (35–47 Å) are usually attributed to the distance between the high affinity Ca^{2+} site and the ATP binding site [28,29]. The shorter (~10 Å) distances may indicate the existence of a Mg^{2+} binding subsite for the binding of Mg-ATP near the ATP binding pocket [26,30–32].

The distances of 10–22 Å between the Eu^{3+} binding site and the catalytic site derived from the quenching of Eu^{3+} luminescence by Cr-ATP [26,33] do not fit readily into either interpretation, suggesting that the position of the Cr atom in the bound Cr-ATP may differ from that of fluorescein or trinitrophenol in the bound FITC or TNP-ATP. In fact the inhibition of ATPase activity by FITC can be overcome by high ATP concentrations [34], suggesting that FITC decreases the affinity of ATP, but does not block the ATP binding site.

Considering the 18 Å length of the ATP molecule, the wide range of estimated distances between the Ca^{2+} and ATP binding sites can accommodate the structural requirements of either direct or indirect coupling mechanisms, and more accurate data are needed to choose between them.

The large (~56–68 Å) distance between AEDANS bound at cysteine-670 and -674 and FITC or TNP-ATP bound at the nucleotide site [35] is of some interest because the AEDANS site may serve as a point of reference for other distance measurements. The only comparable distance in the cytoplasmic domain of the Ca^{2+}-ATPase is the ~60 Å length of the pear-shaped profile shown in Fig. 1. We propose that the binding site for IAEDANS is near the tip of the lobe at a position marked 'D' in Fig. 1, while the site labeled by FITC or TNP-ATP is located at the opposite end of the cytoplasmic domain near the bridge at a site marked 'F' in Fig. 1 [15]. Such a location of the FITC site is consis-

tent with the proposed distance of ~47 Å between FITC and Tb^{3+} bound at the high affinity Ca^{2+} site [29]. To match the 16–18 Å distance between the AEDANS site and the Ca^{2+} binding site [35], the AEDANS site must be positioned on the lower surface of the lobe close to the cytoplasmic surface of the bilayer (position 'D' in Fig. 1).

5. THERMAL FLUCTUATIONS IN THE STRUCTURE OF THE Ca^{2+}-ATPase

Since Ca^{2+} is transferred across the membrane in association with the Ca^{2+}-ATPase, thermal fluctuation of critical regions of the Ca^{2+}-ATPase, perhaps influenced in specific ways through phosphorylation by ATP, may play a role in Ca^{2+} translocation. A similar idea has been proposed some time ago by Huxley [36] in relationship to myosin crossbridge movements, and by Welch et al. [37] on the role of protein fluctuations in enzyme action.

Temperature-dependent changes in the normalized energy transfer efficiency [38] between site-specific donor and acceptor fluorophores indeed reveal structural fluctuations in the Ca^{2+}-ATPase (Fig. 2 and [15]). The temperature dependence of normalized energy transfer efficiency varied depending on the location of the donor-acceptor pairs, suggesting the existence of flexibility gradients within the ATPase molecule.

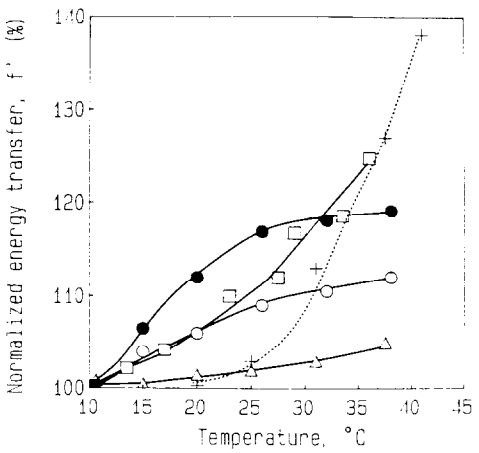

Fig. 2. Temperature dependence of normalized energy transfer, f', for different donor-acceptor systems in sarcoplasmic reticulum. The normalized energy transfer, f' [38], was calculated from the average energy transfer efficiencies, $\langle E \rangle$, determined from steady-state intensity data [15], taking as 100% the values obtained at 10°C for sarcoplasmic reticulum (○,●, □, △) and at 20°C for RNase T_1 (+). Symbols: (○) energy transfer from AEDANS to FITC in the E_1 state (medium: 0.1 M KCl, 30 mM Tris/Mops, pH 7.0, 5 mM $MgCl_2$ + 0.1 mM $CaCl_2$); (●) energy transfer from AEDANS to FITC in the E_2V state (medium: 0.1 M KCl, 30 mM Tris-Mops, pH 7.0, 5 mM $MgCl_2$ + 0.1 mM EGTA, 0.5 mM Na_3VO_4); (□) energy transfer from FITC to Nd^{3+} (1 μM); (△) energy transfer from AEDANS to Pr^{3+} (1 μM); (+) energy transfer data on RNase T_1, a water-soluble protein, using tryptophan as donor and pyridoxamine-phosphate as acceptor; taken from [38] for comparison.

For example, the normalized energy transfer between AEDANS and FITC increased by 13% and 20% in the E_1 and E_2-V states, respectively, upon raising the temperature from 10 to 38°C. Considerable thermal fluctuation of the structure was also evident in the energy transfer between FITC and Nd^{3+}, representing the region of the molecule connecting the ATP binding site (FITC) to the Ca^{2+} channel (Nd^{3+}). By contrast, the region monitored by the AEDANS-Pr^{3+} pair appears to be rigid, judged from the insensitivity of the normalized energy transfer efficiency to temperatures between 10–37°C (Fig. 2).

The increased fluctuation of protein structure at elevated temperatures is reflected in the thermal expansion of proteins [39] and may contribute to the marked temperature dependence of the rate of Ca^{2+} transport.

6. PRESSURE EFFECTS ON SARCOPLASMIC RETICULUM

Interference with structural fluctuations by high (0.5–1.0 kbar) pressure inhibits the Ca^{2+}-ATPase [40] and changes the structure of the enzyme in a conformationally specific manner [13,21,41].

Stabilization of the 'E_2' conformation of Ca^{2+}-ATPase by vanadate and by dimethylsulfoxide provides striking protection against inactivation by 1.5–2.0 kbar pressure [13,21,41]. The protective effect is consistent with a volume decrease of ~200 ml/mol connected with the $E \cdot Ca \longrightarrow E_2$-V transition [41]. Some of the protective effect of vanadate and dimethylsulfoxide against pressure inactivation may be related to the reduced exposure of the cytoplasmic domains of Ca^{2+}-ATPase to water in the E_2 state.

7. THE EFFECT OF MEMBRANE POTENTIAL ON THE STRUCTURE OF Ca^{2+}-ATPase. THE QUESTION OF ELECTRO-CONFORMATIONAL COUPLING

The ATP-dependent Ca^{2+} transport is electrogenic. Artificially imposed membrane potentials of ~100 mV reversibly alter the structure of the Ca^{2+}-ATPase, as indicated by changes in the steady state fluorescence of covalently bound FITC and intrinsic tryptophan [20], and by the effect of membrane potential on the rate of formation and stability of the E_1 and E_2 type Ca^{2+}-ATPase crystals [17,42,43]. Against this background the claim of Tsong [44] that electroconformational coupling may explain the increased Ca^{2+} uptake of sarcoplasmic reticulum vesicles subjected to repeated high voltage pulses, seems plausible. However, analysis of the data presented by Tsong [44] indicates that the observed $^{45}Ca^{2+}$ uptake roughly corresponds to the equilibration of the internal space of sarcoplasmic reticulum (~4 μl/mg protein) with calcium and no active Ca^{2+} uptake took place.

Therefore the high voltage pulses, instead of activating the Ca^{2+} pump, only increased the Ca^{2+} permeability of the membrane, facilitating the passive diffusion of calcium into the vesicles.

8. VANADATE-CATALYZED, CONFORMATIONALLY SPECIFIC PHOTOCLEAVAGE OF THE Ca^{2+}-ATPase

Vanadate (V) interacts with the phosphorylation site of the Ca^{2+}-ATPase as an inorganic phosphate analogue [5,9]. Vanadate-sensitized photocleavage of the Ca^{2+}-ATPase of rabbit sarcoplasmic reticulum was observed upon illumination of sarcoplasmic reticulum vesicles or the purified Ca^{2+}-ATPase by ultraviolet light in the presence of 1 mM monovanadate or decavanadate [23]. The sites of photocleavage were localized in the A tryptic fragment near the T_2 cleavage site in the absence of Ca^{2+} (V site), and in the B tryptic fragment in the presence of 2–20 mM Ca^{2+} (VC site).

In the absence of calcium, vanadate blocks completely the tryptic cleavage of Ca^{2+}-ATPase at the T_2 site [17,45]. Considering the proposed folding patterns of the Ca^{2+}-ATPase [7], the T_2 cleavage site is near the phosphorylation site (Asp-351), where vanadate is likely to be bound. Therefore the proximity of the vanadate binding site to the T_2 cleavage site may explain both the vanadate-catalyzed photocleavage at the V site and the vanadate-induced inhibition of the tryptic cleavage at the T_2 site.

The VC cleavage site in the presence of Ca^{2+} was localized between lysine-515 and aspartate-659 in the general region of the Ca^{2+}-ATPase that contains the ATP binding domain. The high specificity of the cleavage suggests that vanadate bound at a single site may be brought about by conformational changes of the enzyme into reaction either with the V cleavage site in the absence of calcium, or with the VC cleavage site in the presence of calcium. Both sites are likely to be components of the ATP binding/phosphorylation domain.

9. SUMMARY

The conformational changes usually associated with Ca^{2+} transport [9] do not produce readily identifiable changes in the overall shape of the Ca^{2+}-ATPase [17], in the distances between intramolecular markers analyzed by fluorescence energy transfer [14, 15] or in the secondary structure content of the Ca^{2+}-ATPase determined by circular dichroism [10] of FTIR spectrometry [11–13]. Therfore the energy transduction between the phosphorylation site and the Ca^{2+} channel during Ca^{2+} transport probably involves stretching or rotation of helices [1] that alters the vectorial specificity and affinity of the enzyme for ATP, P_i and Ca^{2+}, without changing significantly the content of secondary structures or the overall shape of the ATPase molecule.

A plausible interpretation of the existing data is that the two high affinity Ca^{2+} sites identified by lanthanides are located at ~ 10 Å from each other and ~ 22–47Å from the ATP binding domain [29,33]. Lanthanides also bind to a Mg^{2+} subsite that is within ~ 10 Å from the binding site of TITC [30–31]. The energy transfer data are not sufficiently accurate to permit conclusions about the spatial relationship of the aspartyl phosphate enzyme intermediate or ATP to the transported Ca^{2+}.

High resolution structural data obtainable by X-ray crystallography, and more information about the structural differences between the E and E-Ca^{2+} states of the Ca^{2+}-ATPase are needed to develop a realistic mechanism of the coupling of ATP hydrolysis to Ca^{2+} transport. Recent developments in the crystallization of Ca^{2+}-ATPase [46–49] offer some hope of progress in this direction.

Acknowledgements: Supported by Research Grants AR 26545 from the NIH, PCM 84-03679, 88-23077 and Int. 8617848 from the National Science Foundation and a grant-in-aid from the Muscular Dystrophy Association; N.W.S. receives a postdoctoral fellowship from the NIH (IF32AR0808901), and R.B. from the American Heart Association, New York State Affiliate.

REFERENCES

[1] Tanford, C. (1984) CRC Crit. Rev. Biochem. 17, 123–152.
[2] Mitchell, P. and Koppenol, W.H. (1982) Ann. NY Acad. Sci. 402, 584–601.
[3] Dupont, Y. (1983) FEBS Lett. 161, 14–20.
[4] Scarborough, G.A. (1985) Microbiol. Rev. 49, 214–231.
[5] Inesi, G. and De Meis, L. (1985) in: The Enzymes of Biological Membranes, vol. 3 (Martonosi, A. ed.) pp. 157–191, Plenum Press, New York.
[6] Jencks, W.P. (1989) J. Biol. Chem. 264, 18855–18858.
[7] Green, N.M., Taylor, W.R. and MacLennan, D.H. (1988) in: The Ion Pumps: Structure, Function, and Regulation (Stein, W. ed.) pp. 15–24, Liss, New York.
[8] Clarke, D.M., Loo, T.W., Inesi, G. and MacLennan, D.H. (1989) Nature 339, 476–478.
[9] Dupont, Y., Bennett, N., Pougeois, R. and Lacapere, J.J. (1985) in: Structure and Function of Sarcoplasmic Reticulum (Fleischer, S. and Tonomura, Y. eds) pp. 225–248, Academic Press, Orlando.
[10] Csermely, P., Katopis, C., Wallace, B.A. and Martonosi, A. (1987) Biochem. J. 241, 663–669.
[11] Arrondo, J.L.R., Mantsch, H.H., Mullner, N., Pikula, S. and Martonosi, A. (1987) J. Biol. Chem. 262, 9037–9043.
[12] Villalain, J., Gomez-Fernandez, J.C., Jackson, M. and Chapman, D. (1989) Biochim. Biophys. Acta 978, 305–312.
[13] Buchet, R., Carrier, D., Wong, P.T.T., Jona, I. and Martonosi, A. (1990) Biochim. Biophys. Acta 1023, 107–118.
[14] Birmachu, W., Nisswandt, F.L. and Thomas, D.D. (1989) Biochemistry 28, 3940–3947.
[15] Jona, I., Matko, J. and Martonosi, A. (1990) Biophys. J. 57, 500a.
[16] Dux, L. and Martonosi, A. (1983) J. Biol. Chem. 258, 2599–2603.
[17] Dux, L., Taylor, K.A., Ting-Beall, H.P. and Martonosi, A. (1985) J. Biol. Chem. 260, 11730–11743.

[18] Taylor, K.A., Dux, L. and Martonosi, A. (1986) J. Mol. Biol. 187, 417–427.
[19] Martonosi, A., Taylor, K.A., Varga, S., Ting-Beall, H.P. and Dux, L. (1987) in: Electron Microscopy of Proteins, vol. 6, Membrane Structures (Harris, J.R. and Horne, R.W. eds) pp. 255–376, Academic Press, London.
[20] Jona, I. and Martonosi, A. (1986) Biochem. J. 234, 363–371.
[21] Buchet, R., Jona, I. and Martonosi, A. (1989) Biochim. Biophys. Acta 983, 167–178.
[22] Molnar, E., Seidler, N.W., Jona, I. and Martonosi, A. (1990) Biochim. Biophys. Acta 1023, 147–167.
[23] Vegh, M., Molnar, E. and Martonosi, A. (1990) Biochim. Biophys. Acta 1023, 168–183.
[24] Dux, L. and Martonosi, A. (1983) J. Biol. Chem. 258, 11896–11902.
[25] Scott, T.L. (1988) Mol. Cell. Biochem. 82, 51–54.
[26] Herrmann, T.R. and Shamoo, A.E. (1988) Mol. Cell. Biochem. 82, 55–58.
[27] Teruel, J.A. and Gomez-Fernandez, J.C. (1986) Biochim. Biophys. Acta 863, 178–184.
[28] Highsmith, S. and Murphy, A.J. (1984) J. Biol. Chem. 159, 14651–14656.
[29] Scott, T.L. (1985) J. Biol. Chem. 260, 14421–14423.
[30] Highsmith, S.R. and Head, M.R. (1983) J. Biol. Chem. 258, 6858–6862.
[31] Highsmith, S. (1984) Biochem. Biophys. Res. Commun. 124, 183–189.
[32] Girardet, J.L., Dupont, Y. and Lacapere, J.J. (1989) Eur. J. Biochem. 184, 131–140.
[33] Joshi, N.B. and Shamoo, A.E. (1988) Eur. J. Biochem. 178, 483–487.
[34] Champeil, P., Riollet, S., Orlowski, S., Guillain, F., Seebregts, C.J. and McIntosh, D.B. (1988) J. Biol. Chem. 263, 12288–12294.
[35] Squier, T.C., Bigelow, D.J., Garcia de Ancos, J. and Inesi, G. (1987) J. Biol. Chem. 262, 4748–4754.
[36] Huxley, A.F. (1957) Progr. Biophys. Biophys. Chem. 7, 255–318.
[37] Welch, G.R., Somogyi, B. and Damjanovich, S. (1982) Progr. Biophys. Mol. Biol. 39, 109–146.
[38] Somogyi, B., Matko, J., Papp, S., Hevessy, J., Welch, G.R. and Damjanovich, S. (1984) Biochemistry 23, 3403–3411.
[39] Frauenfelder, H., Hartmann, H., Karplus, M., Kuntz, D.I., Jr., Kuriyan, J., Parak, F., Petsko, G.A., Ringe, D., Tilton, R.F. Jr, Connolly, M.L. and Max, N. (1987) Biochemistry 26, 254–261.
[40] Konig, K.G. and Hasselbach, W. (1984) Z. Naturforschung 39c, 282–288.
[41] Varga, S., Mullner, N., Pikula, S., Papp, S., Varga, K. and Martonosi, A. (1986) J. Biol. Chem. 261, 13943–13956.
[42] Dux, L. and Martonosi, A. (1983) J. Biol. Chem. 258, 11903–11907.
[43] Beeler, T.J., Dux, L. and Martonosi, A. (1984) J. Membr. Biol. 78, 73–79.
[44] Tsong, T.Y. (1988) Methods Enzymol. 157, 240–251.
[45] Dux, L. and Martonosi, A. (1983) J. Biol. Chem. 258, 10111–10115.
[46] Pikula, S., Mullner, N., Dux, L. and Martonosi, A. (1988) J. Biol. Chem. 263, 5277–5286.
[47] Taylor, K.A., Mullner, N., Pikula, S., Dux, L., Peracchia, C., Varga, S. and Martonosi, A. (1988) J. Biol. Chem. 263, 5287–5294.
[48] Stokes, D.L. and N.M. Green (1990) Biophys. J. 57, 1–14.
[49] Stokes, D.L. and N.M. Green (1990) J. Mol. Biol. 213, 529–538.